Journal of Structural Geology 31 (2009) 615–626

Contents lists available at ScienceDirect

Journal of Structural Geology

journal homepage: www.elsevier.com/locate/jsg

Magmatic diapirism of the Fangshan pluton, southwest of Beijing, China

Bin He [a,*], Yi-Gang Xu [a], Scott Paterson [b]

[a] Key Laboratory of Isotope Geochronology and Geochemistry, Guangzhou Institute of Geochemistry, Chinese Academy of Sciences, Guangzhou, Guangdong 510640, China
[b] Department of Earth Sciences, University of Southern California, Los Angeles, USA

ARTICLE INFO

Article history:
Received 2 May 2008
Received in revised form
20 April 2009
Accepted 21 April 2009
Available online 3 May 2009

Keywords:
Magmatic diapirism
Magma ascent
Pluton emplacement
Reworking of host rock
Fangshan pluton

ABSTRACT

Diapirism as a crustal magma ascent and emplacement mechanism has been increasingly questioned due to lack of unambiguous natural examples. In this paper we report the structure of the Cretaceous Fangshan pluton in the hinterland of the North China Craton, ca. 40 km southwest of Beijing, China. This pluton is a compositionally and texturally concentrically zoned granodiorite with an approximately circular shape. Our detailed structural and petrological investigations reveal a high-temperature shear aureole with pluton-side-up kinematic indicators and a rim syncline around the pluton. In addition, an intensely deformed Archean complex occurs at the northern and southern margins of the pluton requiring at least 4 km upward movement through the 4–5 km thick overlying cover sequence during magma ascent. Based on comparison of stratigraphic units inside and outside the aureole, the bulk wall-rock shortening by ductile flow is estimated to be about 4 km, which is roughly the same as the radius of the pluton. These features are consistent with results of numerous modeling studies and diagnostic criteria of magmatic diapirism, indicating that the Fangshan pluton is a magmatic diapir intruded into a ductile upper crust.

1. Introduction

The ascent and emplacement of granitic magmas in the crust have been an enigma in the Earth sciences. Over the past few decades it has been suggested that this process mainly involves complex physical interactions, i.e., material transfer processes of both multiple batches of magmas and host rocks (Buddington, 1959; Paterson and Fowler, 1993). Although fabrics within plutons may provide some information about ascent or/and emplacement, the main clues for material transfer processes should come from the host rocks (Buddington, 1959; Paterson and Fowler, 1993). Some geologists maintain that more may be learned about the granite bodies by studying the enveloping rocks than studying the granites themselves (e.g., Sylvester et al., 1978). Magma ascent and emplacement rework or modify host rock and its structure. Therefore the inverse problem of deducing magma ascent and chamber construction mechanisms may be undertaken by examining the reworking of host rock around the plutons (Zak and Paterson, 2006).

Diapirism, one of the oldest hypotheses of magma ascent and pluton emplacement, is increasingly challenged (Bateman, 1984; Petford, 1996; Clemens, 1998; Petford et al., 2000). During the 1970–90s, numerous theoretical and experimental modeling studies suggested that magmatic diapirs could form in the crust (e.g., Dixon, 1975; Marsh, 1982; Cruden, 1988, 1990; Mahon et al., 1988; Schmeling et al., 1988; Weinberg and Podladchikov, 1994). Some geologists even established diagnostic criteria of granitic diapirs (e.g., Bateman, 1984; Castro, 1987; England, 1990; Brown, 1994; Clemens, 1998). However, despite some publications describing magmatic diapirs (England, 1992; Miller and Paterson, 1995; Paterson and Vernon, 1995; Galadi-Enriquez et al., 2003), other geologists argued that there is little unambiguous evidence for such diapirs in nature (Bateman, 1984; Petford, 1996; Clemens, 1998; Petford et al., 2000).

The Fangshan pluton is located northwest of Fangshan town, ca. 40 km southwest of Beijing, China (Fig. 1). This pluton and its wall rocks are very well exposed and have been extensively studied from a geological, geochemical and geochronological perspective since 1936 (e.g., Ho, 1936; Ma, 1989; Zhang and Li, 1990; BGMRBM, 1991; Ma et al., 1996; Cai et al., 2005). In this paper, our detailed structural and petrological investigations reveal an inner high-temperature shear aureole with pluton-side-up kinematic indicators and an outer aureole dominated by a rim syncline around the pluton. Below we present observations that lead us to conclude that the Fangshan pluton is a good example of a magmatic diapir.

2. Geologic setting and regional structures

The Fangshan area lies in the hinterland of the North China Craton (NCC) (Fig. 1). This craton consists of Archean and Early

* Corresponding author. Tel.: +86 2085290855; fax: +86 2085290420.
E-mail address: hebin@gig.ac.cn (B. He).

0191-8141/$ – see front matter © 2009 Elsevier Ltd. All rights reserved.
doi:10.1016/j.jsg.2009.04.007

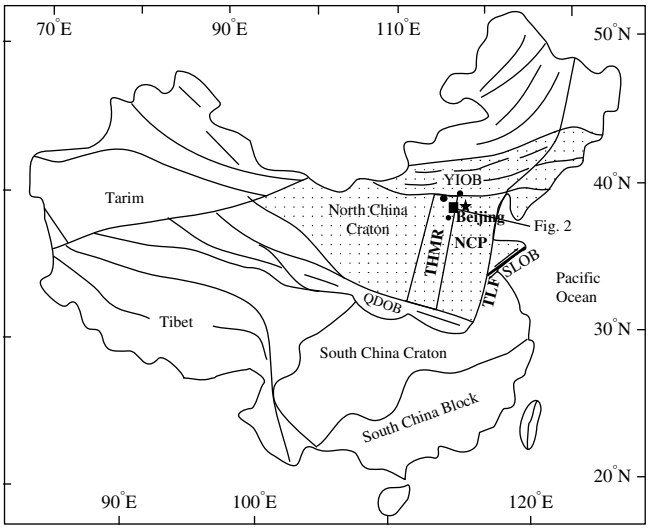

Fig. 1. Map showing general geology of China and the location of the Fangshan area. Three black circular dots in the Fangshan area are locations where the thickness of Proterozoic strata has been measured. YIOB, Yanshan Intraplate Orogenic Belt; THMR, Taihuang Mountains Range; QDOB, Qingling-Dabie Orogenic Belt. SLOB, Sulu Orogenic Belt; NCP, North China Plain; TLF, Tan-Lu Fault.

Proterozoic crystalline basement covered by a passive margin sequence, which continued to exist until the Jurassic (BGMRBM, 1991) at which time the NCC was tectonically reactivated and developed strong deformation and voluminous Mesozoic magmatism resulting in the E–W trending Yanshan intraplate orogenic belt along its northern edge (Fig. 1).

2.1. Regional stratigraphy

The NCC basement is Archean and Lower Proterozoic, consisting mainly of higher grade metamorphic rocks such as gneiss, amphibolites, and leptynite. The cover sequence includes 3–6 km thick Meso- to Neoproterozoic (ca. 1800–800 Ma) shallow marine strata, Cambrian–Middle Ordovician shallow marine carbonates, and Upper Carboniferous–Permian marine and terrestrial coal-bearing clastic rocks. The Late Permian rocks are unconformably overlain by Lower Triassic red-beds and conglomerates, which in turn, are unconformably overlain by Mesozoic volcanic and clastic deposits (BGMRBM, 1991).

The stratigraphy preserved in the Fangshan area is nearly the same as in the broader NCC. Sequences of the cover are the Mesoproterozoic Changcheng Group (Pt_2Ch), Jixian Group (Pt_2Jx), Neoproterozoic Qingbaikou Group (Pt_3Qb), Paleozoic Cambrian, Lower Ordovician, Carboniferous, Permian, Triasic, and Jurassic (Table 1). The following three observations from these sequences are important for our study: (1) the stratigraphic formations are lithologically consistent, and easily recognizable in field mapping; (2) the thickness of Middle and Upper Proterozoic strata in this area is about 4 km as inferred from the iso-thickness maps (BGMRBM, 1991); and (3) Pre-Mesozoic units in this area were metamorphosed under greenschist facies conditions (BGMRBM, 1991) in contrast to unmetamorphosed cover in other parts of the NCC.

Another important element of the local stratigraphy occurs at the southern and northern margins of the Fangshan pluton (Figs. 2, 3 and 5). Here, higher grade metamorphic rocks such as gneiss, amphibolite, migmatic gneiss, migmatite, leptynite and their corresponding tectonites (i.e., mylonites and straight gneiss) occur in tectonic slices, forming a complex of tectonic slices. The idiomorphic zircons from the granitic gneiss in the complex have a Pb–Pb age around 2449 Ma (Wang and Chen, 1996) and SHRIMP U–Pb zircon age at 2521 ± 20 Ma (Yan et al., 2006), indicating that these rocks are Archean.

2.2. Structures and deformation sequences of the Fangshan area

The most striking structural features in this area are bedding-parallel ductile structures (D_1), which are developed in the

Table 1
Summary of stratigraphic units in the Fangshan area (BGMRBM, 1991).

Chronostratigraphy			Formations	Symbol	Thickness (m)	Main rocks
Erathem	System	Series				
Mesozoic	Cretaceous			K	1134	Sandstone, siltstone
	Jurassic			J	~2100	Clastic rocks
	Triassic			T	246	Shale and siltstones
Upper Paleozoic	Permian	Upper	Hongmiaoling	P_2h	54–178	Sandstone
		Lower	Shihezi	P_1sh	29–58	Siltstone and shale
			Shanxi	P_1s	37	Siltstone and sandstone
	Carboniferous	Upper	Taiyuan	C_3t	47	Sandstone, shale
		Middle	Benxi	C_2b	43.78	Sandstone, shale
Lower Paleozoic	Ordovician	Lower		O_1	440	Limestone
	Cambrian	Upper		$\in_3$	50	Mud-limestone
		Middle		$\in_2$	117	Slate, limestone
		Lower		$\in_1$	115	Dark gray limestone
Upper Proterozoic	Qingbaikou	Pt_3Qb	Jingeryu	Pt_3j	135–202	White marble
			Changlongshan	Pt_3ch	60–120	Quartzose sandstone
			Xiamaling	Pt_3x	300	Shale and slate
Middle Proterozoic	Jixian	Pt_2Jx	Tieling	Pt_2t	212	Dolomite with flints
			Hongshuizhuang	Pt_2h	101	Shale and slate
			Wumishan	Pt_2w	2239	Dolomite with flints
			Yangzhuang	Pt_2y	76	Limestone
	Changcheng	Pt_2Ch	Gaoyuzhuang	Pt_2g	991	Shale and limestone
			Dahongyu	Pt_2d	445	Feldspar sandstone
			Tuanshanzi	Pt_2t	59	Domolite
			Chuanlinggou	Pt_2ch	49	Silty sandstone
			Changzhougou	Pt_2c	1057	Quartzose sandstone
Archean				ArG	>200	Gneiss and amphibolite

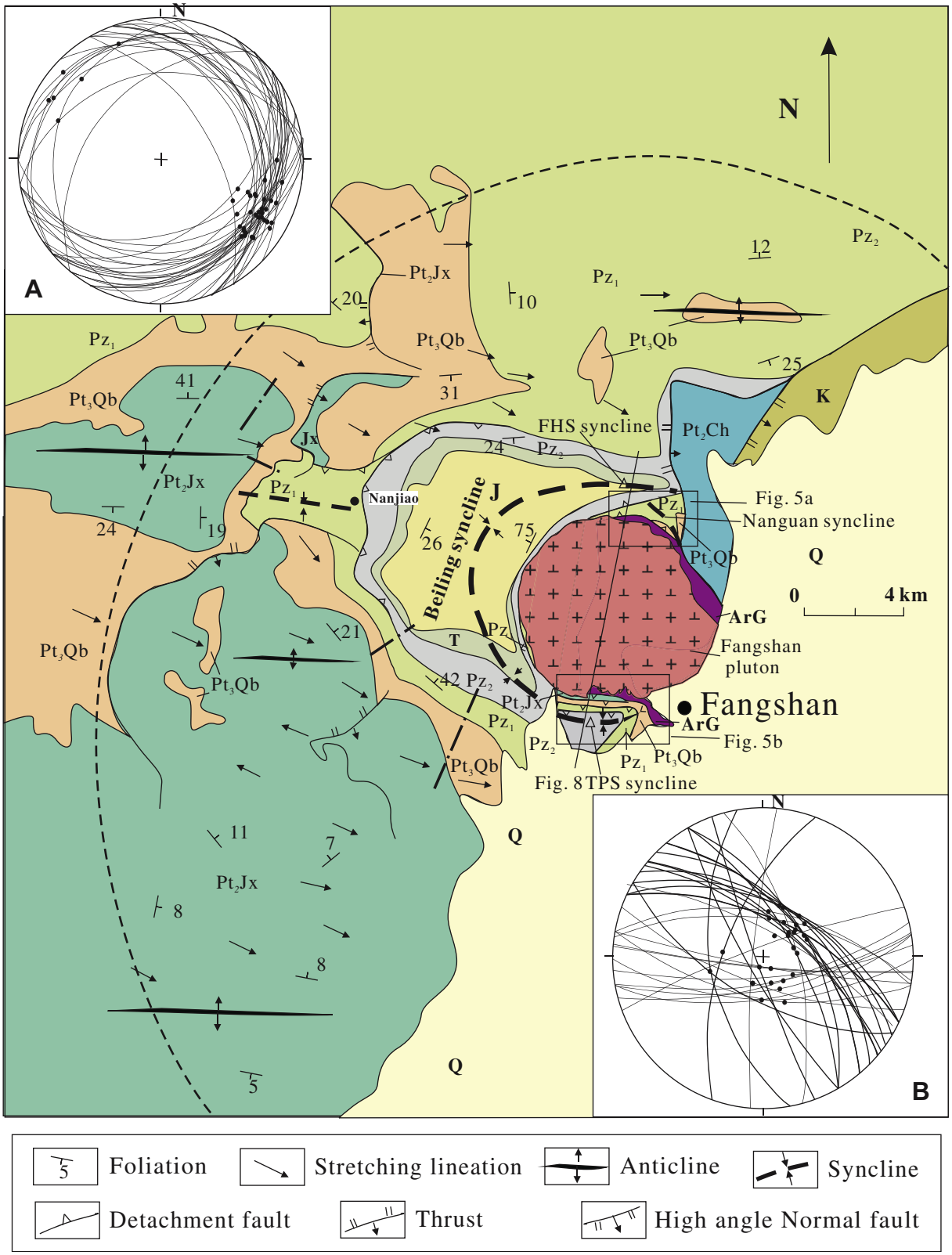

Fig. 2. Map of the regional geology in the Fangshan area (modified from Song et al., 1996). Stratigraphic units and their symbols: Archean Guandi complex (ArG), Mesoproterozoic Changcheng group (Pt_2Ch), Jixian group (Pt_2Jx), Neoproterozoic Qingbaikou System (Pt_3Qb); Lower Paleozoic (Pz_1), Upper Paleozoic (Pz_2), Triassic (T), Jurassic (J), Cretaceous (K), Quaternary (Q) (more descriptions are shown in Table 1). Insert A and B are Schmidt diagrams (lower hemisphere) of regional foliation (great circles) and of stretching lineation (dots) in the high-temperature shear aureole (HTSA) around the Fangshan pluton respectively. Note that the stretching lineations in the HTSA (Insert B) are radial and steep, whereas the foliations are concentric and steep. The regional stretching lineations beyond the HTSA (Insert A) are NW–SE trending with gently dipping strata. The dashed line roughly marks the limit of early ductile flow structures. Dash-dotted lines are locations where stratigraphic units are measured. TPS – Taipingshan; FHS – Fenghuangshan.

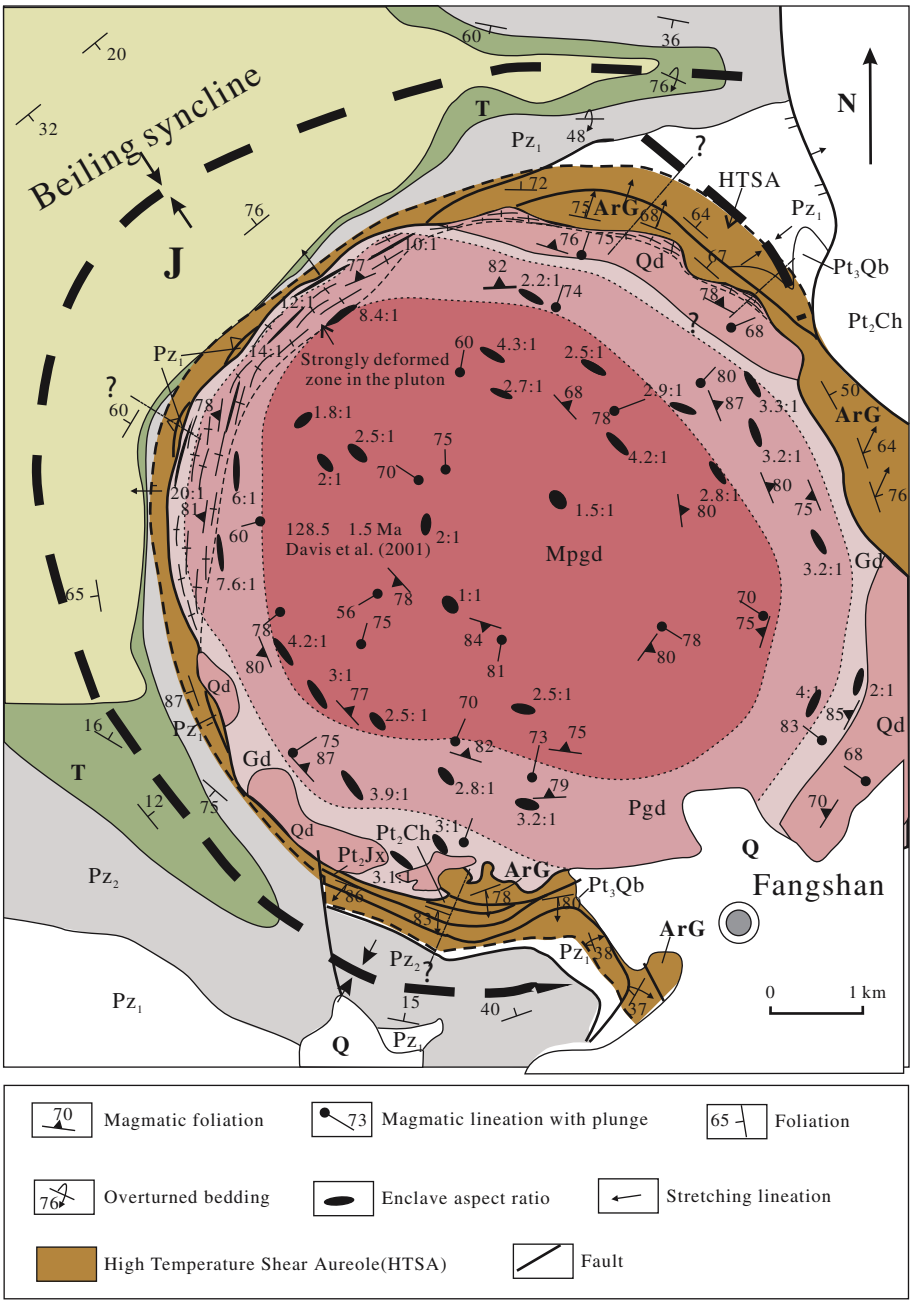

Fig. 3. Structural and geological map of the Fangshan pluton and its wall rocks. Symbols of stratigraphic units are the same as those in Fig. 2. The pluton has four units: fine-grained quartz diorites (Qd), medium-grained granodiorites (Gd), porphyritic granodiorites (Pgd) and megaporphyritic granodiorites (Mpgd). Dashed line roughly marks the exterior boundary of HTSA of the Fangshan pluton. Dotted line defines the internal boundary within the pluton of subsolidus deformation. Dash-dotted lines with numbers are locations of structural sections shown in Fig. 6.

Pre-Mesozoic cover (Song, 1987). The ductile structures consist of bedding-parallel ductile shear zones, intrafolial to inter-formational recumbent folds and transposition of bedding during formation of a continuous foliation (Song, 1996; Song et al., 1996). The distribution of these ductile structures forms a roughly semi-circular area, centered on the Fangshan pluton, with a diameter of 50 km (Fig. 2) (Song and Zhu, 1997). Stretching lineation is well developed with a consistent plunge of SE 110–130° (Insert A in Fig. 2). Strain analysis using different markers (e.g., oolite, pebbles) indicates that the strain was mainly simple shear in the center of the ductile domain, and pure shear at its margin (Song and Zhu, 1997). S–C fabrics, mica-fish, quartz axis fabrics among others indicate that the sense and direction of ductile shear is top-to-SE (Song and Wei, 1990; Song and Zhu, 1997).

Pre-Mesozoic cover in this area underwent regional greenschist facies dynamo-thermal metamorphism (e.g., Wang and Ma, 1989; Song, 1996). The common mineral assemblage in the metapelitic rocks is muscovite, chlorite, chloritoid and quartz, indicating a metamorphic temperature between 250 and 400 °C (Wang and Ma, 1989). The metamorphic regime is centered, just as is the ductile domain, on the Fangshan pluton and forms a semi-circular area with a diameter of 60 km, 10 km larger than the diameter of the ductile structure domain (Song and Zhu, 1997).

Ar–Ar dating of 5 muscovite samples in the ductile domain indicates that greenschist facies metamorphism took place during the Early Cretaceous (128.7–150.2 Ma, B. He, unpublished). This metamorphic age is a little earlier than but close to the age of the Fangshan pluton (i.e., 128.5 ± 1.5, Davis et al., 2001) (see Section 3.2). Although the geometrical, kinematic, temporal and spatial distribution of the ductile structures have been well studied, its geodynamic origin is still not well understood.

After the emplacement of the Fangshan pluton (D_2), three other deformation events (D_3–D_5) occurred: broad E–W trending anticlines (D_3), a tight syncline in the Nanjiao area 12 km northwest of the Fangshan pluton, thrust faults (D_4) and their associated NE-trending folds overprinting E–W trending folds at Nanjiao, and a high-angle normal fault (D_5) in the eastern part of the Fangshan pluton (Figs. 2 and 3). This fault strikes NNE and dips 70–85° to the ESE. The block west of the pluton is composed of Proterozoic to Paleozoic strata, whereas Cretaceous to Quaternary sediments of the North China Plain occur on the east side.

Despite the numerous deformation events, the general structural pattern in this area, outside of the rim syncline and high strain aureole of the Fangshan pluton, is rather simple. Strata generally dip gently (5–25°) throughout the area (Fig. 2).

3. Description of the Fangshan pluton

3.1. Internal units

The 58 km^2 Fangshan pluton has an approximately circular map pattern with a diameter of 7.5–9 km (Fig. 3). The pluton is a concentrically zoned diorite–granodiorite complex composed of two separate pulses resulting in four mappable units (Fig. 3) (Ma, 1989; Ma et al., 1996; Cai et al., 2005). Field observations indicate that two pulses have clear cross-cutting relationships. The older pulse is fine-grained quartz diorite (Qd), and occurs as small bodies along the northern and southern margins of the pluton and in a large exposed body along the eastern margin of the pluton. As the eastern margin is covered by thick Cenozoic sediments, its boundary is not well constrained. The younger pulse can be subdivided into three units from the margins inwards: medium-grained granodiorite (Gd), porphyritic granodiorite (Pgd) and megaporphyritic granodiorite (Mpgd) (Fig. 3). These three units tend to be concentric (Fig. 3). Contacts between these three units are gradational over distances of up to 260 m. Microgranular dioritic and gabbroic enclaves and lamprophyric dykes occur in the pluton (Ma et al., 1996).

3.2. Geochronology

Most existing geochronological data were obtained from the granodiorite, which was dated ca. 132 Ma by biotite and hornblende K–Ar and Ar–Ar methods in different laboratories both in China and Australia (Ma, 1989). Recently, SHRIMP U–Pb ages of zircons from the granodiorite were determined as 128.5 ± 1.5 Ma (Davis et al., 2001) and 130 ± 1.4 Ma (Cai et al., 2005). One published K–Ar whole rock age from quartz diorite at the southern margin of the pluton is ca. 131.1 Ma (BGMRBM, 1991), LA-ICP-MS U–Pb ages of 28 zircons from fine-grained quartz diorite (Qd) north of the pluton give an age of 132.4 ± 1.3 Ma (B He, unpublished, 2007) representing the age of the oldest intrusional pulse.

3.3. Geochemistry

The four units of the Fangshan pluton are chemically homogeneous (Cai et al., 2005): their major element compositions are characterized by high Na_2O (4.06 ~ 6.8) and high Na_2O/K_2O ratio (1.11 ~ 2.80). The rocks are enriched in LREE and depleted in HREE, and have no Eu anomaly, δEu = 0.9–1.16. The pluton is high in Sr (1113 ~ 1640 ppm), Sr/Y (75 ~ 222) and La/Yb ratios (21–149), but low in heavy rare-earth elements (HREEs; Yb ≤ 1.7 ppm) and Y (≤15.6 ppm), resembling within plate adakites (Cai et al., 2005). The geochemical signatures indicate that the melts formed at least at 40 km depth (1.2 GPa) (Rapp and Watson, 1995; Petford and Atherton, 1996). The geochemical data combined with Sr–Nd isotopic compositions ($^{87}Sr/^{86}Sr = 0.7056$–0.7058; $^{143}Nd/^{144}Nd = 0.5118$–$0.5119$) suggest that the adakites were formed by partial melting of the newly (early-Mesozoic) underplated, mafic lower crust (Cai et al., 2005).

3.4. Emplacement depth of the pluton

The Fangshan pluton intrudes Permian strata along its western margin, the maximum thickness of overlying strata of the pluton (i.e., from Permian to Early Cretaceous) being about 3 km (Table 1) (BGMRBM, 1991). On this basis the estimated intrusion depth of the pluton, using techniques similar to Sylvester et al. (1978) for the Papoose Flat pluton, is about 3 km. However, based on sillimanite–K-feldspar barometry in country rocks, pressure of emplacement is estimated at about 2 kb corresponding to a depth of about 6 km (Deng, 1978). This difference in emplacement depth may be caused by overpressure during final emplacement or upward displacement after the formation of sillimanite–K-feldspar assembly.

3.5. Magmatic foliation and lineation

Magmatic foliation, defined by the alignment of hornblende, biotite, tabular feldspar and oblate enclaves is present throughout the pluton (Fig. 3). In general, the foliation intensity decreases from the margin to the center of the pluton. Foliation in the pluton is steep and parallel with that in the structural aureole, showing a circular pattern (Fig. 3). Magmatic lineation, defined by preferred alignment of hornblende crystals, feldspars and elongated enclaves observed in the magmatic foliation is also present throughout much of the pluton. Most magmatic mineral lineation plunges about 60–85° towards the country rock. But in the southern part of the pluton, they often plunge inwards at angles of about 75–85°.

3.6. Enclave fabrics

Microgranitoid enclaves are widespread in the intrusion and are typically oblate. Generally, the number and oblateness of the enclaves increase gradually towards the pluton margins, and the oblate planes tend to be parallel to foliation on the margins, although some notable exceptions occur (Fig. 3). On average, enclave aspect ratios decrease regularly with the distance from the contact, and vary from more than 5/1–1.5/1, being largest (up to 8/1 up to 21/1) at the NW margin of the pluton (Zhang and Li, 1990).

3.7. Subsolidus deformation in pluton

Subsolidus deformation occurs, as the name implies, after magmatic solidification and is mainly localized along the western and northern margins of the pluton (dotted line, Fig. 3), the eastern margin not being exposed. An arcuate, moderately deformed zone, occurs along the NW margin of the pluton (Fig. 3). This zone is about 6 km long and 200–600 m wide. It is characterized by the presence of structures related to some subsolidus deformation, including elongated enclaves and secondary small shear zones. Within 100–200 m of the wall-rock contact in this zone, a type of S–C-like structure occurs (Fig. 4A); the S surface represents the modified initial magmatic foliation, the C surface forms discrete

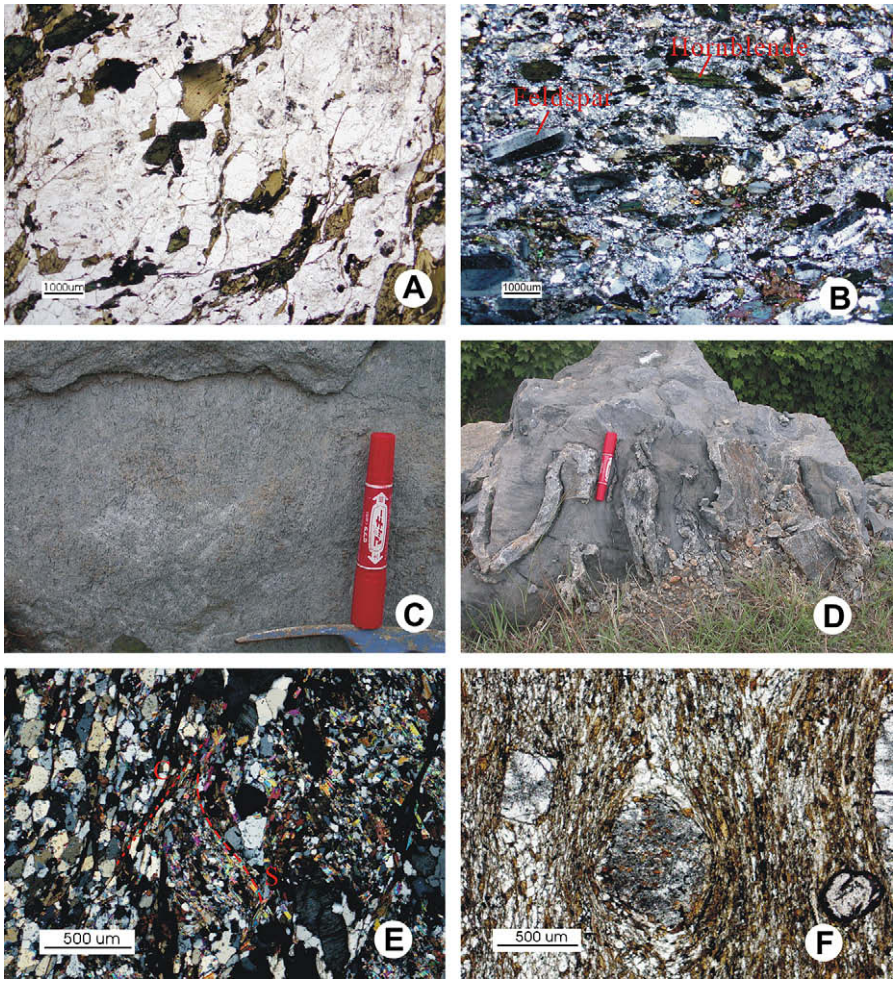

Fig. 4. Field photos and photomicrographs of the Fangshan pluton and its aureole. (A) S–C fabric of deformed granodiorite in the western part of the pluton, note ductile deformation of biotites in plane polarized light; (B) Subgrains or dynamic recrystallization of feldspars and elongated hornblends of diorite from the northern margin of the pluton (cross-polarized light); (C) Preferred alignment of tremolite causing a steeply plunging mineral lineation in strongly deformed marble from the southern aureole of the pluton; (D) steeply plunging fold hinge of small intrafolial complex folds in marble of the southern aureole of the pluton, viewed down the steeply fold plunge; (E) S–C fabric of quartz schist in the southern margin; (F) photomicrographs of rocks in HTSA from the southern margin of the pluton; note andalusite and garnet porphyroblasts with internal inclusion trails at variable angles to the matrix foliation.

lenticular 1–4 mm thick and several centimeters long shear zones. Locally, rocks in this arcuate zone are mylonitic, the enclaves in the pluton are pancake-shaped with the flat plane being parallel to the gneissosity and to the aureole foliation, and all dipping 85°. Subsolidus deformation decreases in intensity across the zone towards the center of the pluton. Later minor or small discrete shear zones are superimposed on this deformation, which usually develops in pairs and in combination forms conjugate shear zones with the obtuse bisectrix perpendicular to the gneissosity and to the aureole. The rocks in the ductile zones are mylonites with S–C fabric, subhorizontal mineral lineations, and metamorphic honrnblende.

A narrow, intensely developed, subsolidus deformation zone (several to tens of meters wide) occurs near the northern host–wall contact, parallel with the host–pluton contact. Subgrains or dynamic recrystallization of feldspars and elongated hornblendes of rocks in this zone are observed, implying that it is a high-temperature shear zone (Fig. 4B) with steep subsolidus lineation. In some localities, S–C fabrics of this zone show pluton-side-up vertical movement. No structures related to subsolidus deformation are observed in the southern margin of the pluton. However, foliated structures indicative of subsolidus deformation in dikes in the aureole along this margin were documented (Song and Wei, 1990).

4. The thermal and structural aureole

4.1. The thermal aureole

The Fangshan pluton intruded a variety of host rocks including Archean gneisses, Proterozoic dolomite, Lower Paleozoic limestone and pelite, Upper Paleozoic clastic rocks and pelite, forming a 300–2000 m wide contact metamorphic zone around the pluton. Hornfels, schists, marbles, and gneisses are common, and most have strong foliations and lineations. Contact metamorphism to the west of the Fangshan pluton may be divided into an andalusite–K-feldspar, andalusite, and andalusite–biotite zone, corresponding to metamorphic temperatures of 690–730, 575–690, and 450–575°C respectively (Wang and Chen, 1996).

4.2. General features of the structural aureole

A structural aureole, with variable thickness, is well developed around the Fangshan pluton. This aureole has an inner high temperature, high strain aureole, designated HTSA, and large rim syncline in the outer edge of aureole (Fig. 3). The aureole varies in structural style around the pluton perimeter. Along the southern

margin of the pluton, aureole deformation is manifested by extreme thinning and attenuation of strata in addition to local folding and faulting of Archean slices (Fig. 5b). Stratigraphic units in this part of the aureole are tectonically and concordantly thinned to as little as 10% of their regional thickness without loss of stratigraphic identity (see below). Along the northern margin of the pluton, a slice of Archean rocks progressively thrusts from east to west, in fault contact with the Xiamaling Fm., Jingeryu Fm. and Cambrian and Ordovician units (Fig. 5a). To the west, the pluton intruded Upper Paleozoic clastic rocks, forming a narrow deformation aureole in which limited thinning of stratigraphic units is recognized. A rim syncline is well developed along the outer margin (Figs. 2 and 3).

4.3. Host rock–pluton contact

A sharp contact tends to exist between the Fangshan pluton and its wall rocks. This host rock–pluton interface is relatively straight along the western margin of the pluton, where host rock is mainly Upper Paleozoic and Jurassic. The contact is stepped or zigzagging and thus complex along the southern and northern margins of the pluton (Figs. 3 and 5). Especially in zones where quartz diorite

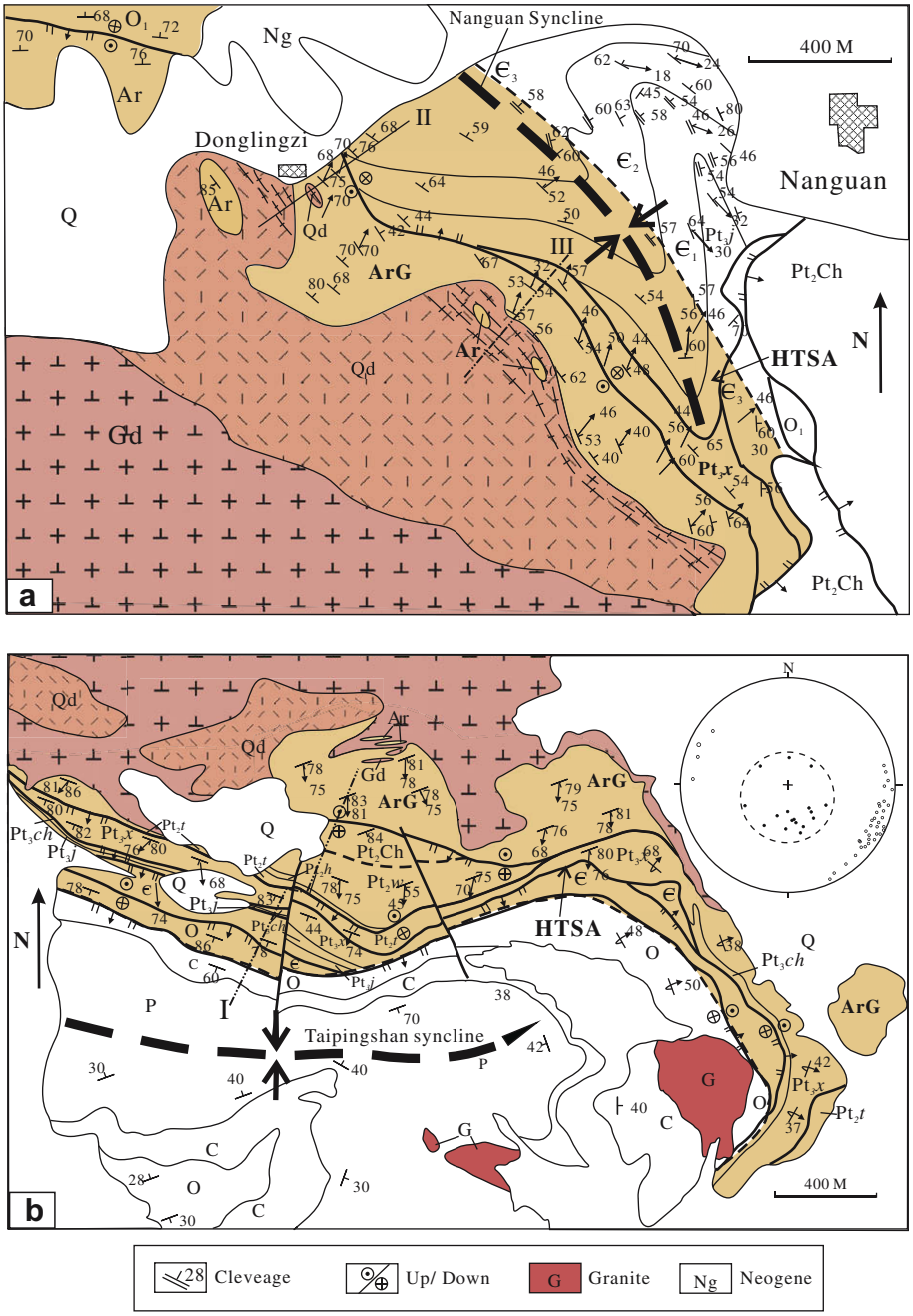

Fig. 5. Detailed structural maps of aureoles around the north (a) and south (b) of the Fangshan pluton. The areas are shown in Fig. 2. Symbols of stratigraphic units are the same as Table 1. Legends are as Fig. 3 unless otherwise indicated. Insert in Fig. 5b is a Schmidt diagram (lower hemisphere) of hinges of small intrafolial folds in the HTSA around the south of the Fangshan pluton (dots in dashed line circle) and in region (hollow dots). Note that lineations dip steeply northeast (Fig. 5a) at the northern aureole and south at the southern aureole.

intruded the Archean slices, host rock–pluton contacts are irregular and locally gradational. Locally small Archean blocks or xenoliths occur in the margin of the pluton and in the small quartz diorite bodies in the Archean gneiss (Figs. 5 and 6). In both cases, the Archean rocks are strongly deformed whereas the adjacent intrusive diorite has a mainly magmatic fabric.

4.4. High temperature, high strain aureole (HTSA) in the inner aureole

Most of rocks in the inner HTSA are strongly foliated and lineated and are typical S–L tectonites. The pervasive foliation is steep (60–88°), dips away from the pluton and is usually concordant to the pluton/wall-rock contact (Fig. 3). This foliation is also subparallel to bedding. Foliation dip gradually decreases outwards in the aureole. A stretching lineation is well developed in the aureole, and is defined by aligned tremolite (Fig. 4C), andalusite, sillimanite, elongate quartz and mica assemblage, and plunges steeply (60–84°) (Figs. 2–4C). This aureole lineation is subparallel with the magmatic lineation in the pluton and differs from the regional NW–SE trending, gently plunging (5–25°) stretching lineation (Insert A in Fig. 2) associated with greenschist facies grade minerals in the regional deformation zone. Complex intrafolial folds whose hinges, without exception, plunge steeply (Insert in Fig. 5b) are seen in many outcrops of banded marbles (Fig. 4D). As the intrafolial recumbent folds of early bedding-parallel ductile folds strike consistently SE 110–130° outside this zone, these complex folds with steep hinges are interpreted as being the result of vertical stretching of the aureole during the plutonic emplacement. In the HTSA, fold hinges are slightly oblique or parallel to the shear sense direction, implying that the inner aureole had a large component of vertical stretching and/or shear. Boudins are common in marbles and schists and commonly folded. Some boudins also preserve hook-like folds.

Rocks in the HTSA are mainly strongly deformed mylonites, gneiss, schist and banded marbles. In some thin sections from the HTSA, two or three generations of foliation occur (Fig. 4E, F). An early gently dipping foliation is preserved in micro-fold hinges and as inclusion trails in porphyroblasts and is thought to represent pre-emplacement regional deformation. The dominant foliation in the matrix, which wraps porphyroblasts, is interpreted to represent the steep foliation related to emplacement of the pluton. Curvature of initial foliations in porphyroblasts into the steeply dipping foliation indicates that the transposition of the older foliation into steep orientations occurred during porphyroblast growth. Fibrolite is sometimes less well aligned, suggesting late growth and aureole deformation prior to fibrolite formation.

Kinematic indicators within the aureole at all scales show a consistent kinematic sense. In map view, four normal faults in the southern aureole (Fig. 5b), asymmetrical folds, and tectonic lens within fault zones clearly indicate pluton-side-up vertical movement. In outcrop scale, S–C fabrics and secondary shear zones are observed within the aureole. In one exposure of the southern aureole, granite veins in Xiamaling Formation schist have S–C fabrics, indicating pluton-side-up movement sense. S–C fabrics and mica-fish texture in thin sections from the mylonites within the aureole also show pluton-side-up vertical movement.

4.5. Thinning and absence of stratigraphic units in the structural aureole

The well-established regional stratigraphy allows us to study the thinning and/or removal of stratigraphic units in the structural aureole. We compared regional stratigraphic thicknesses outside of the Western Hill deformation zone to those within this zone but outside the aureole and to those within the structural aureole. Especially along the southern margin of the pluton (Figs. 5b–7), stratigraphic units in the HTSA are thinned to as little as 10% of their regional thickness without loss of stratigraphic identity. To quantitatively study thinning of stratigraphic unit thickness, a cross section was measured at the south end of the Fangshan pluton (profile I in Fig. 3, results in profile I Fig. 6 and column B and D in Fig. 7). We made the following three inferences based on these profiles: (1) more than 4 km stratum was removed through

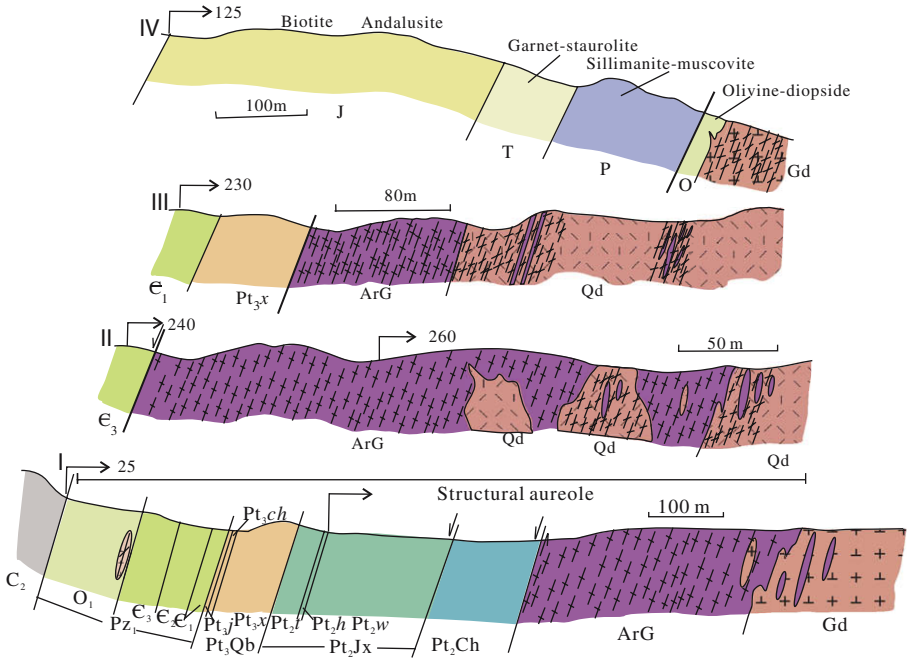

Fig. 6. Structural sections of the HTSA around the Fangshan pluton. Locations of sections are shown in Figs. 3 and 5. Symbols of stratigraphic units and legends are the same as those in Figs. 2, 3 and 5.

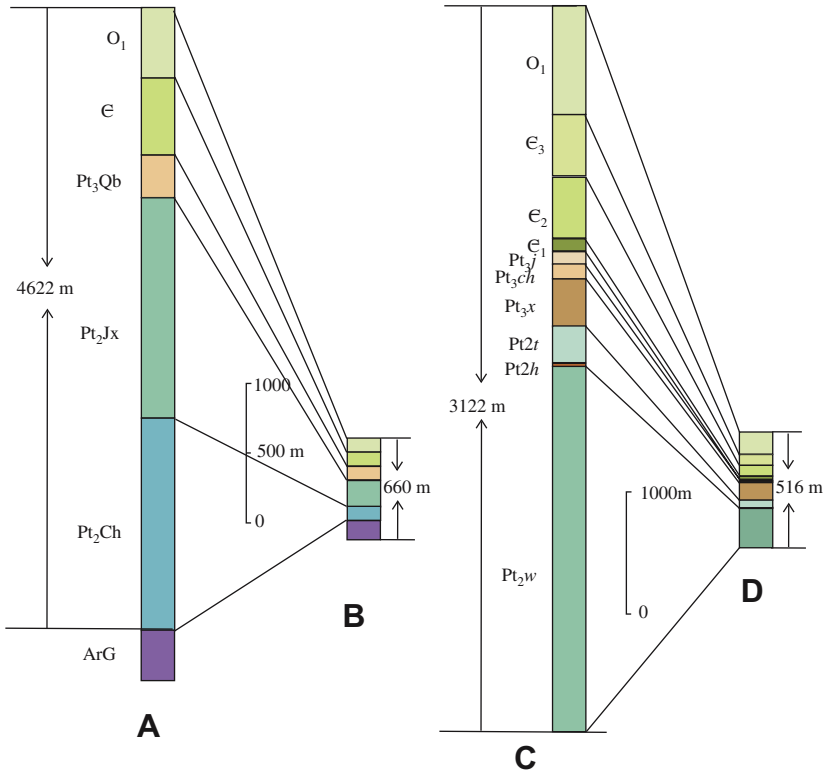

Fig. 7. Thickness comparison between interior and exterior strata of HTSA. Thickness of Upper Proterozoic and Paleozoic estimates in Sections A and C are from 4 km southwest of the Fangshan pluton (locations are marked in Fig. 2); thickness of Mesoproterozoic Changcheng Group and Jixian Group are taken from the smallest thicknesses in three adjacent sections in Fig. 1. Sections B and D are from profilelin HTSA of the southern margin of the pluton (location is indicated in Figs. 3 and 5).

thinning within this aureole. In other words, bulk wall-rock shortening at the southern margin of the pluton is about 4000 m; (2) with increasing distance from the pluton, thinning decreases sharply. Outward thinning from the pluton by stratigraphic unit is: Changcheng Group 95%, Jixian Group 85%, Qingbaikou Group 60%, Paleozoic units 50%; (3) incompetent units thin more than competent units. For example, Jingeryu Formation (marble, from 60–200 m to 1 m) of Qingbaikou group thins more than the Longshan Formation quartzite (20–60 m to 15–10 m).

Absence, and thus inferred removal, of some stratigraphic units occurs in the structural aureole. In the western margin of the pluton, detailed field mapping reveals that the Ordovician is in contact with Permian (Fig. 6, profile 4), implying that the Carboniferous Taiyuan and Benxi Formations are completely removed. This loss of units occurs only 2 km away from the NW margin of the pluton (Fig. 3). At the southern margin, the Archean is in direct contact with the Upper Proterozoic Xiamaling Formation (Fig. 5b). Fig. 5a also shows that Ordovician units are in normal fault contact with the Archean implying removal of the Proterozoic and Cambrian. This geometry indicates that a large amount of aureole displacement occurred on discrete fault surfaces.

4.6. Rim syncline around the pluton

Bordering the pluton is a well developed rim syncline (Figs. 2 and 3). The syncline is asymmetric in cross section (Fig. 8), has thinner strata and steeper dips (85–60°) adjacent to the pluton. Locally some strata at the flank of the pluton are overturned; the other limb of the syncline has thicker strata and gentler dips (15–30°) (Fig. 8). The syncline hinge line and the map traces of the axial planar cleavage are both parallel to the pluton contact. This rim syncline is overprinted by a thrust nappe in the northeast. Near the SW margin of the pluton the synclinal hinge line steepens as it approaches the margin of the Fangshan pluton (Figs. 2 and 5b). The rim syncline is separated into four locally named synclines: Nanguan, Fenghuangshan, Beiling and Taipingshan synclines from northeast to southeast (Fig. 2). The large topographic relief (>1000 m) in this area allowed us to examine vertical changes in these synclines, because it intersects the syncline at different depth. Thus the Nanguan syncline occurs at 100 m elevation and represents the deepest part of the syncline, the Taipingshan syncline at 250 m the intermediate, and the Fenghuangshan syncline at 700 m, the top part. Our examination indicates that the wavelength tightens with depth within these synclines.

5. Discussion

5.1. Characteristics of magmatic diapirism and its comparison with ballooning

Emplacement mechanisms for roughly circular, zoned plutons are mainly considered to be ballooning (e.g., Sylvester et al., 1978; Bateman, 1984; Ramsay, 1989) and diapirism (e.g., Marsh, 1982; Cruden, 1988, 1990; Mahon et al., 1988; Schmeling et al., 1988; Weinberg and Podladchikov, 1994; Paterson and Vernon, 1995). Generally speaking, diapirism is defined as the upward movement of magma into (non-piercing) or through (piercing) overlying rocks; whereas ballooning is the relatively symmetrical, radial expansion of magma chamber where the center of the magma chamber does not move significantly relative to a far-field reference frame (Paterson and Vernon, 1995). These different models are difficult to distinguish in many cases. It seems from modeling and some natural examples, that magmatic diapirs may go through a ballooning stage during their emplacement (e.g., Dixon, 1975; England, 1990, 1992; Galadi-Enriquez et al., 2003).

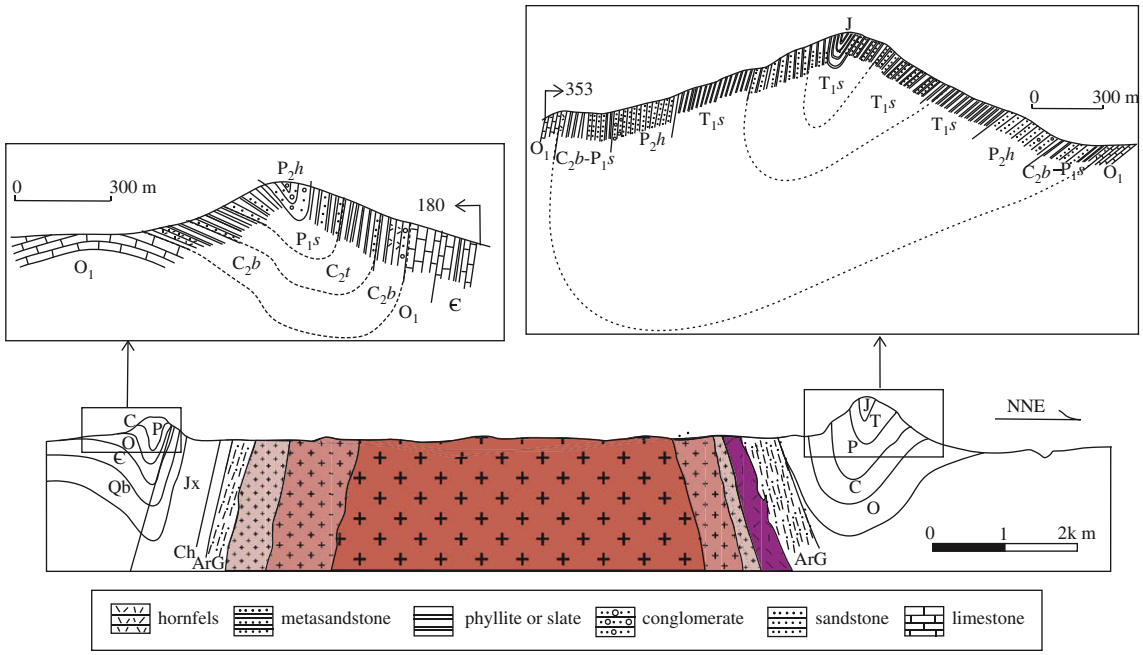

Fig. 8. Structural sections of the Taipingshan and Fenghuangshan synclines around the Fangshan pluton. Locations of sections are shown in Fig. 2. Stratigraphic units: C_2b – Carboniferous Benxi Fm.; C_2t – Carboniferous Taiyuan Fm.; P_1s – Permian Shanxi Fm.; P_2h – Permian Hongmiaoling Fm.; T_1s – Triassic Shuangquan Fm.

Some geologists designate magmatic diapirs as ballooning diapirs (e.g., Ramsay, 1989; Bateman, 1984). However, most geologists think that the distinctive feature of ballooning is that it occurs *in situ*, with magma ascent potentially transported by dykes. This makes ballooning very different from diapirism in that magmatic diapirism requires vertical displacement of country rocks, a high-temperature shear aureole with steep lineation and pluton-side-up kinematic indicator, and an asymmetrical rim syncline, whereas a ballooning pluton causes flattening deformation of country rock (Table 2). Thus examining the deformation and structures of host rocks distinguishes diapirism from ballooning.

5.2. Evaluation of ballooning mechanism for the Fangshan pluton

The Fangshan pluton has many characteristics in common with roughly circular zoned plutons exposed at middle- to upper-crustal levels throughout the world. These include: (1) a sub-circular shape in plan view; (2) multiple sub-concentric intrusive phases; (3) concentric fabrics within the pluton and its aureole, local solid-state zones of deformation along its margin; (4) locally concordant and locally discordant contacts with compositional and deformational layering in wall rocks around the pluton; and (5) strong deflection of wall rocks within a generally narrow deformation aureole. This suite of features is consistent with *in situ* expansion or "ballooning of a magma chamber" (e.g., Sylvester et al., 1978; Bateman, 1984; Ramsay, 1989). Because of these features earlier Chinese geologists have suggested that the Fangshan pluton was emplaced by ballooning. They included in their assessment also the average increase of 2D enclave aspect ratios with distance from the pluton center and the subsolidus deformation in local zones along the plutonic margin (Wang and Ma, 1989; Zhang and Li, 1990; Ma et al., 1996).

However a number of our observations are not in accordance with an *in situ* ballooning model. Among these are the following three specific ones: (i) the structural aureole of the pluton records large-scale vertical displacement and removal of stratigraphic units, (ii) both pluton and aureole preserve a steeply plunging mineral stretching lineation, and (iii) kinematics in the aureole and locally in the pluton indicate vertical motions.

Cruden (1990) noted that flattening strain could occur at the margins of magmatic diapirs. Therefore, the existence of such flattening strain at the margins of the Fangshan pluton does not preclude diapirism. We also did not find evidence of strictly flattening strain in host rocks. Ultimately without exposure of the pluton floor and geophysical data, there will always remain some ambiguity with respect to ballooning for the Fangshan pluton.

Table 2
Characteristics of host rocks for magmatic diapir and its comparison with ballooning (after Clemens, 1998; England, 1990; Miller and Paterson, 1995).

	Magmatic diapir	Ballooning	The Fangshan pluton
Stretching Lineations	Radial and steep	None	Radial and steep
Foliations	Concentric	Concentric	Concentric
High-T shear aureole	Yes	No	Yes
Vertical displacement	Yes	No	Yes
Rim syncline	Yes, asymmetrical	Likely, symmetrical	Yes, asymmetrical
Strain type	Shearing and flattening	Flattening	Shearing

5.3. Diapir mechanistic evaluation for the Fangshan pluton: is the Fangshan pluton a magmatic diapir?

As we discussed above, the main clues for magma ascent and pluton emplacement should come from the host rocks (e.g., Buddington, 1959; Paterson and Fowler, 1993). Our detailed structural and petrological investigations show the following features of host rocks as depicted in the piercing scenario shown in Fig. 9: (1) an inner HTSA with dominantly pluton-side-up kinematics; (2) a concentric pattern of steeply dipping foliations and radial steeply plunging stretching lineations in the inner HTSA; (3) slices of Archean rocks at northern and southern margins implying at least

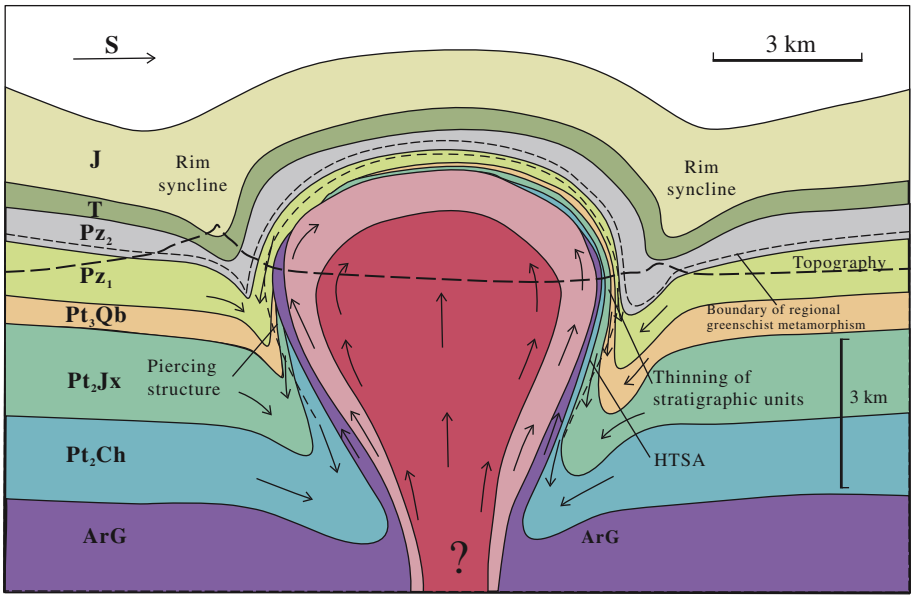

Fig. 9. Emplacement model of the Fangshan pluton illustrating the inner HTSA, concentric pattern of steeply dipping foliations, slices of Archean rocks, outer rim syncline and wavelength tightening of the syncline with depth.

4 km vertical displacement; and (4) an outer zone of rim synclines. These observations are in accordance with both theoretical and experimental modeling (e.g., Dixon, 1975; Marsh, 1982; Cruden, 1988, 1990; Mahon et al., 1988; Schmeling et al., 1988; Weinberg and Podladchikov, 1994), and predictions for magmatic diapirism (Bateman, 1984; Castro, 1987; England, 1990; Brown, 1994; Clemens, 1998). Another test for magmatic diapir is to compare the magnitude of the bulk wall-rock shortening to the size of the pluton, addressing the plutonic emplacement "space problem" (Clemens, 1998). As noted earlier the bulk wall-rock shortening at the southern margin of the pluton is about 4000 m, which is roughly the same as the radius of the pluton, indicating that this shortening meets all space requirements for this pluton by diapirism (Fig. 7). The above considerations lead us to interpret the Fangshan pluton as a magmatic diapir intruded into ductile upper crust (Fig. 9; Table 2).

We noted before that diapirism as a crustal magma ascent and emplacement mechanism has been increasingly questioned due to lack of unambiguous natural examples. The present study presents fairly compelling evidence that diapirism remains a plausible emplacement mode for this pluton. At present, we can only constrain the vertical ascent distance to roughly 4 km based on the occurrence of Archean fragments at the northern and southern margins of the pluton, and the unperturbed stratigraphic 4–5 km cover sequence. It remains unclear whether the magma ascended from its melting depth (40 km) entirely as a diapir.

6. Summary

We report the structure of the Fangshan pluton and the deformation of its host rocks, southwest of Beijing, China. Our detailed structural and petrological investigations reveal a high-temperature shear aureole with pluton-side-up kinematic indicators and a rim syncline around the pluton. These features are consistent with results of numerous theoretical and experimental modeling on magmatic diapir, providing compelling evidence that the Fangshan pluton is a magmatic diapir intruded into ductile upper crust.

Acknowledgments

This study was supported by the National Science Foundation of China (40672140). We are grateful to the reviewers for their constructive reviews and suggestions. Professor de Jong took care of linguistic issues. Some ideas in this paper originated in discussions with Professors Song and Davis.

References

Bureau of Geology and Mineral Resources of Beijing Municipality (BGMRBM), 1991. Regional Geology of Beijing Municipality. Geological Publishing House, pp. 1–598 (in Chinese with English abstract).
Bateman, R., 1984. On the role of diapirism in the segregation, ascent and final emplacement of granitoid magmas. Tectonophysics 10, 211–231.
Brown, M., 1994. The generation, segregation, ascent and emplacement of granite magma, the migmatite-to-crustally-derived granite connection in the thickened orogens. Earth Science Reviews 36, 83–100.
Buddington, A.F., 1959. Granite emplacement with special reference to North America. Geological Society of American Bulletin 70, 671–747.
Cai, J.H., Yan, G.H., Mu, B.L., Reng, K.X., Song, B., Li, F.T., 2005. Zircon U–Pb age, Sr–Nd–Pb isotopic compositions and trace element of Fangshan complex and their petrogenesis significance. Acta Petrologica Sinica 21, 776–788 (in Chinese with English abstract).
Castro, A., 1987. On granitoid emplacement and related structures – a review. Geologische Rundschau 76, 101–124.
Clemens, J.D., 1998. Observations on the origins and ascent mechanisms of granitic magmas. Journal of the Geological Society of London 155, 843–851.
Cruden, A.R., 1988. Deformation around a rising diapir modeled by creeping flow past a sphere. Tectonics 7, 1090–1101.
Cruden, A.R., 1990. Flow and fabric development during the diapiric rise of magma. Journal of Geology 98, 681–698.
Davis, G.A., Zheng, Y., Wang, C., Darby, B.J., Zhang, C., Gehrels, G., 2001. Mesozoic tectonic evolution of Yanshan fold and thrust belt, with emphasis on Hebei and Liaoning provinces, Northern China. Geological Society of American Memoir 194, 171–197.
Deng, J.F., 1978. Thermodynamic calculations for metamorphic reactions involved in the formation of sillimanite-hornfels around the Fangshan pluton. Geochimica 3, 234–241 (in Chinese with English abstract).
Dixon, J.M., 1975. Finite strain and progressive deformation in models of diapiric structures. Tectonophysics 28, 89–102.
England, R.W., 1990. The identification of granitic diapers. Journal of the Geological Society of London 147, 931–933.
England, R.W., 1992. The genesis, ascent, and emplacement of the North Arran Granite, Scotland, implications for granitic diapirism. Geological Society of American Bulletin 104, 606–614.
Galadi-Enriquez, E., Galindo-Zaldivar, J., Simancas, F., Exposito, I., 2003. Diapiric emplacement in the upper crust of a granitic body, the La Bazana granite (SW Spain). Tectonophysics 361, 83–96.

Ho, T.L., 1936. The granitic intrusions of the Western Hills of Beijing. In: Book Series of Geological House, Central Academy, vol. 5, pp. 1–15.
Ma, C.Q., 1989. The magma-dynamic mechanism of emplacement and compositional zonation of the Zhoukoudian stock, Beijing. Acta Geologica Sinica 2, 159–173 (in Chinese with English abstract).
Ma, C.Q., Wang, R.J., Chen, N.S., 1996. Magmatic thermodynamic structures of the Zhoukoudian granodioritic intrusion in the Western Hills of Beijing. In: Field Trip Guide of 30th International Geological Congress. Geological Published House, Beijing, p. 14.
Mahon, K.I., Harrison, T.M., Drew, D.A., 1988. Ascent of a granitoid diapir in a temperature varying medium. Journal of Geophysical Research 93, 1174–1188.
Marsh, B.D., 1982. On the mechanics of igneous diapirism, stoping and zone melting. American Journal of Sciences 282, 808–855.
Miller, R.B., Paterson, S.R., 1995. In defense of magmatic diapers. Journal of Structural Geology 21, 1161–1173.
Paterson, S.R., Fowler, T.R.J., 1993. Re-examining pluton emplacement processes. Journal of Structural Geology 115, 191–206.
Paterson, S.R., Vernon, R.H., 1995. Bursting the bubble of ballooning plutons, a return to nested diapirs emplaced by multiple processes. Geological Society of American Bulletin 107, 1356–1380.
Petford, N., 1996. Dykes and diapirs? Transactions of the Royal Society of Edinburgh, Earth Sciences 87, 105–114.
Petford, N., Atherton, M., 1996. Na-rich partial melts from newly underplated basaltic crust, the Cordillera Blanca batholith, Peru. Journal of Petrology 37, 1491–1521.
Petford, N., Cruden, A.R., McCaffrey, K.J.W., Vigneresse, J.L., 2000. Granite magma formation, transport and emplacement in the earth's crust. Nature 408, 669–673.
Ramsay, J.G., 1989. Emplacement kinematics of a granitic diapir, the Chinamora batholith. Journal of Structural Geology 11, 191–210.
Rapp, R.P., Watson, E.B., 1995. Dehydration melting of metabasalt at 8–32 kbar, implications for continental growth and crust–mantle recycling. Journal of Petrology 36, 891–931.
Schmeling, H., Cruden, A.R., Marquart, G., 1988. Finite deformation in and around a fluid sphere moving through a viscous medium, implication for diapiric ascent. Tectonophysics 149, 17–34.
Song, H.L., 1996. Characteristics of Fangshan metamorphic core complex, Beijing and a discussion about its origin. Geoscience 10, 147–158 (in Chinese with English abstract).
Song, H.L., 1987. A primary analysis on the tectonic sequence in the southern part of the western hill, Beijing. Earth Science 12, 15–20 (in Chinese with English abstract).
Song, H.L., Fu, Z.R., Yan, D.P., 1996. Extensional tectonics and metamorphic core complex of the Western Hills of Beijing. In: Field Trip Guide of 30th International Geological Congress. Geological Published House, Beijing, pp. 1–8.
Song, H.L., Wei, B.Z., 1990. Metamorphic core complexes and their significance in the continental crustal evolution. Geoscience 1, 111–121 (in Chinese with English abstract).
Song, H.L., Zhu N., 1997. Mesozoic geothemal anomaly in western hills of Beijing and origin of Fangshan metamorphic core complex. In: Proceedings of the 30th International Geological Conference, vol. 14, pp. 149–157.
Sylvester, A.G., Oertel, G., Nertel, C.A., Christie, J.M., 1978. Papoose flat pluton, a granitic blister in the Inyo Mountains, California. Geological Society of American Bulletin 89, 1205–1219.
Wang, F.Z., Chen, N.S., 1996. Regional and thermodynamic metamorphism of the Western Hills of Beijing. In: Field Trip Guide of 30th International Geological Congress. Geological Published House, Beijing, pp. 1–10.
Wang, R.J., Ma, C.Q., 1989. Features and emplacement of the Zhoukoudian stock, Beijing. Earth Science 14, 399–406 (in Chinese with English abstract).
Weinberg, R.F., Podladchikov, Y., 1994. Diapiric ascent of magmas through power law crust and mantle. Journal of Geophysical Research 99, 9543–9560.
Yan, D.P., Zhou, M.F., Song, H.L., Wang, G.H., Sun, M., 2006. Mesozoic extensional structures of the Fangshan tectonic dome (Beijing, North China) and their subsequent deformation. Journal of the Geological Society of London 163, 127–142.
Zak, J., Paterson, S.R., 2006. Roof and walls of the Red Mountain Creek pluton, eastern Sierra Nevada, California (USA), implications for process zones during pluton emplacement. Journal of Structural Geology 28, 575–587.
Zhang, J.S., Li, Z.Z., 1990. Emplacement deformations and ballooning mechanism about Fangshan granodiorite pluton, Beijing. In: Zhang, J.S. (Ed.), The Geological Study of Xishan, Beijing. China University of Geosciences Press, Wuhan, pp. 48–63 (in Chinese with English abstract).